Research on Engineering Structures & Materials
www.jresm.org
Research Group

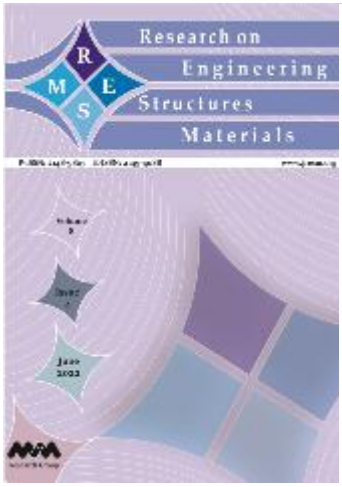

Response surface methodology use in optimization of concrete properties using blast furnace slag aggregate and recycled concrete sand

Poonam, VP Singh

Online Publication Date: 30 September 2023
URL: http://www.jresm.org/archive/resm2023.788me0614.html
DOI: http://dx.doi.org/10.17515/resm2023.788me0614
Journal Abbreviation: *Res. Eng. Struct. Mater.*

To cite this article
Poonam, Singh VP. Response surface methodology use in optimization of concrete properties using blast furnace slag aggregate and recycled concrete sand. *Res. Eng. Struct. Mater.*, 2024; 10(1): 111-133.

Research on Engineering Structures & Materials
www.jresm.org
Research Group

Research Article

Response surface methodology use in optimization of concrete properties using blast furnace slag aggregate and recycled concrete sand

Poonam*, [a], VP Singh[b]

Department of Civil Engineering, National Institute of Technology, Kurukshetra, (Haryana) India

Article Info

Article history:

Received 14 June 2023
Accepted 27 Sep 2023

Keywords:

Regression equations;
BFSA replacement;
RCS replacement;
Split tensile strength;
Bond strength

Abstract

The utilization of waste materials in concrete plays a crucial role in sustainable construction by contributing to environmental conservation and enhancing concrete properties. However, waste management and sustainable construction present significant challenges within the construction industry. This study specifically focuses on the optimization of concrete properties by utilizing Blast furnace slag aggregate (BFSA) as coarse aggregate (CA) and recycled concrete sand (RCS) as fine aggregate (FA). To assess the impact of BFSA and RCS replacement parameters, response surface methodology (RSM) based on central composite design (CCD) was employed. The RSM regression equations generated in this study demonstrated high R2 values (>0.8), indicating their capability to explain the variability observed in the responses. To assess the impact of BFSA and RCS replacement parameters, response surface methodology (RSM) based on central composite design (CCD) was employed. In conclusion, the implementation of RSM enables the incorporation of waste materials into concrete, resulting in waste reduction without significant effects on concrete properties.

1. Introduction

Rapid urbanization and industrialization have led to an increase in construction and demolition (C&D) waste generation, resulting in a higher demand for natural resources [1]. The disposal of C&D waste through dumping and landfilling causes environmental issues and land occupation. Reclaiming C&D waste is crucial for reducing end-of-life impacts and minimizing the extraction of natural resources [2–4]. Recycling C&D waste into aggregates, particularly as sustainable building materials, has been extensively studied, and it has been accepted that recycled coarse aggregates (RCAs) can replace natural coarse aggregates by up to 30% without sacrificing concrete performance [5–7]. However, a significant portion of concrete fines still cannot be recycled and reused. Recycled concrete powder (RCP) has been investigated as a replacement for fine aggregate in mortar or concrete. Studies have shown that RCP mortar exhibits inferior properties due to higher porosity and water absorption [8,9]. The inclusion of RCP affects the particle packing status of aggregates in mortar, primarily due to changes in particle size distribution after adding different contents and sizes of RCP particles. The packing status of granular materials can be characterized by the particle packing density, which is defined as the absolute volume to bulk volume ratio of the packed material.

Various industrial by-products, including red mud, fly ash, silica fume (SF), metakaolin, B flexural strength, and rice husk ash, have been used as cement replacements to enhance

*Corresponding author: poonam_6170006@nitkkr.ac.in
[a] orcid.org/0009-0002-2153-512X; [b] orcid.org/0009-0002-2153-512X
DOI: http://dx.doi.org/10.17515/resm2023.788me0614

concrete strength [9–13]. These by-products possess latent hydraulic properties, leading to improved compressive strength (CS) at an early stage and flexural strength at a later age. Incorporating these by-products into concrete helps conserve natural resources. The utilization of ground granulated blast furnace slag (GBFS), a by-product of the iron-making process, has gained significant attention. Blast furnace slag is a versatile material with a structure similar to conventional building materials such as cement and natural stone. It can be recycled and used in a variety of ways, such as replacing cement, improving concrete, and even making bricks. The cooling method during production affects how we can use it. When a molten slag is rapidly cooled with water, the result is a granular aggregate. This granular material is mainly processed as ground granulated blast furnace slag aggregate which is known as Granulated Blast furnace slag Aggregate (BFSA), which is commonly used in various construction projects, including mixed and precast concrete, masonry, floor level materials, and high temperature resistant building manufacturing processes. GBFS has high glass content and potential hydration activity when rapidly cooled by water quenching [14]. It has been widely used in the cement and concrete industry, as well as in other applications [15].

The utilization of solid wastes for the production of composite ground granulated blast furnace slag (GBFS) as an alternative to natural coarse has been investigated in previous studies [16,17]. The promotion of GBFS hydration is facilitated by the synergistic effects of solid wastes and flexural strength, which encompass alkali, sulphate, and particle filling effects. Composite GBFS not only caters to the need for superior quality GBFS, but also facilitates the efficient usage of many other solid waste materials, hence fostering collaboration across different industries. Several research works have investigated the utilization of GBFS and Recycled Concrete Aggregate (RCA) in the context of concrete. The utilization of self-compacting concrete (SCC) with GBFS as a substitute for natural coarse aggregate resulted in a significant decrease in compressive strength, surpassing 20% as reported in previous studies [18,19].

Previous research conducted on blast furnace slag aggregate concrete has demonstrated the potential for enhancing the compressive strength, flexural strength, and split tensile strength of the concrete. Qasrawi [20] did a study on the utilization of furnace slags as coarse aggregate in concrete constructions. The findings indicated that including furnace slag as a coarse aggregate in concrete has the potential to enhance the mechanical characteristics of the concrete. Maslehuddin et al. [21] conducted an assessment of the mechanical properties and durability characteristics of furnace slag aggregate concrete and normal aggregate concrete. The experimental findings demonstrated that the durability properties of concrete containing furnace slag aggregate surpassed those of concrete containing normal aggregate. Additionally, certain mechanical attributes of furnace slag aggregate concrete, including compressive strength, flexural strength, and split tensile strength, exhibited improvements in comparison to normal aggregate concrete. The authors Yu et al. [22] undertook a series of experiments to investigate the properties of concrete with steel slag and waste glass. The findings of the study suggest that the substitution of coarse aggregate with steel slag and/or waste glass is a viable option. BFSA concrete exhibits considerable potential as a feasible alternative to concrete including natural aggregate within the building sector [23]. Nevertheless, a significant portion of the prior research has mostly concentrated on the application of BFSA as the fine aggregate. Several studies [24-26] have examined the behavior of coarse aggregate with a significant volume replacement of natural aggregates. Some of these studies [27] have specifically focused on determining the behavior in question. Multiple studies have demonstrated that the physical properties of concrete with BFS aggregates closely resemble those of concrete incorporating naturally occurring aggregates [11].

1.1. Response Surface Methodology

An efficient method is required for optimizing the properties of concrete containing waste materials, as it is an important step towards sustainable construction that reduces the depletion of natural resources and promotes cleaner neighborhoods [28]. RSM has been used to generate models for independent variable optimization, which is a statistical, theoretical, and numerical technique [45,46]. The effect of independent parameters on one or numerous responses is considered by RSM, which employs partial factorial designs like CCD to generate response surfaces for second-order mathematical models [29]. Mathematical models generated using RSM have been observed to be efficient in predicting the properties of concrete containing waste materials [30].

Several researchers have applied the use of RSM in the optimization of concrete containing waste materials, and it has been found to be an effective method for identifying mixtures that yield the best compromises among the responses [31,32]. Regression analysis, experimental designs, and recommended statistical tests are generated by RSM employing design of experiment (DOE) software packages such as Minitab and Design Expert [33]. Partial factorial designs used by RSM reduce the number of experiments required compared to full factorial designs, making it a practical method for researchers with limited time and resources [34].

Numerous investigations have been undertaken to examine the mechanical characteristics of concrete by substituting natural resources with various waste materials [35]. Additionally, diverse contemporary methodologies have been employed for the purpose of optimization [36]. Although there have been research investigations examining the substitution of river sand with WFS in regular concrete mixtures [37], there is a lack of statistical modeling and optimization of concrete mixtures that incorporate WFS. Based on the extant study data, it can be inferred that Response Surface Methodology (RSM) has the potential to serve as a valuable tool for determining the optimal proportion of Waste Foundry Sand (WFS) to be utilized as a replacement for natural sand in concrete. This may be achieved by employing a design matrix that incorporates relevant parameters and corresponding responses. In order to address the existing research gap, the present study aimed to examine the slump and mechanical properties of a concrete mixture. This was achieved by partially replacing the fine aggregate with varying percentages of WFS. The experimental design matrix was built using the CCD function of RSM. During the experimental design, the factors chosen were the WFS percentage and number of curing days, while the responses picked were the CS, STS, and FS. The water-to-fly ash ratio incrementally increased from 0% to 40% in intervals of 10%, while the duration of the curing process ranged from 7 to 56 days. The concrete mixtures were formulated based on the recommended proportions of water, fine aggregate, and coarse aggregate. The corresponding characteristics of the concrete were assessed at designated time intervals, as specified by the experimental design matrix [38]. The statistical models were afterwards constructed through the utilization of ANOVA analysis, allowing for the examination of the combined impacts of various factors on the specified responses. Ultimately, the process of multi-objective design optimization was undertaken in accordance with predetermined design criteria in order to ascertain the optimal proportion of WFS and the duration of curing days that would yield the highest levels of slump and mechanical properties. The optimal outcomes that were acquired were then validated using further experimental procedures.

A solution to cost-effective conventional concrete production is provided by this study using waste materials such as BFSA (0-50%) as coarse aggregate and RCS (0-100%) as sand replacement in concrete. The performance of concrete containing these waste materials is predicted by mathematical models generated in this study, which optimize

their contents split tensile strength and flexural strength [39]. The response surface models generated in this research are distinct from those developed by other researchers and validate the practicability of the generated models. Overall, an efficient method that can bring about a revolution in sustainable construction is the use of RSM in optimizing the properties of concrete containing waste materials [40,41].

1.2. Optimization Process

The optimization process for the RSM based on CCD involves finding the optimal values of BFSA and RCS replacement percentages to achieve the desired response variable while considering any constraints that may exist. The first step is to generate a mathematical model using experimental data and validate it through ANOVA [41,42] . Once the model is validated, optimization techniques can be employed to determine the optimal values of the input variables (BFSA and RCS) for the desired response variable. Various optimization techniques can be used, such as RSM, gradient-based optimization, or genetic algorithms. Response surface plots can help visualize the relationship between the input variables and the response variable, aiding in the identification of optimal values. Constrained optimization techniques consider any constraints, such as cost limitations or specific strength requirements. These techniques find optimal values that satisfy the constraints while achieving the desired response [30,36]. To verify the optimal values, experiments can be conducted at the predicted values, and the results can be compared to the model predictions. If the experimental results align with the model predictions, the optimal values are considered the final solution. If discrepancies occur, the model may require refinement or additional experiments for improved accuracy. Over the last decade, there has been a growing trend towards employing optimal experimental designs as opposed to traditional methods. This shift is attributed to their enhanced flexibility and capacity to address a broader spectrum of challenges compared to conventional designs [39].

The study presents significant opportunities for sustainable construction through the utilization of Blast furnace slag aggregate (BFSA) and recycled concrete sand (RCS). However, it exhibits certain gaps. Firstly, the investigation into the long-term durability and performance of concrete mixes incorporating BFSA and RCS is lacking, requiring future exploration. Additionally, a comprehensive environmental assessment, involving life cycle analysis, is necessary to holistically evaluate the sustainability impact of these materials in concrete. Moreover, to effectively scale up the adoption of waste materials in concrete construction, bridging the divide between research findings and practical implementation, while addressing industry standards and regulations, remains a vital challenge. The study aims to optimize concrete properties by incorporating Blast Furnace Slag Aggregate (BFSA) as coarse aggregate and Recycled Concrete Sand (RCS) as fine aggregate. This involves utilizing Response Surface Methodology (RSM) and Central Composite Design (CCD) to assess how different levels of BFSA and RCS replacements impact split tensile strength, flexural strength, and bond strength. The research demonstrates that this approach enables the integration of waste materials into concrete, promoting sustainable construction practices by reducing waste while maintaining concrete quality, as evidenced by high R^2 values in regression equations.

2. Materials and Methods

2.1. Materials

In this study, the researchers used 43-grade OPC cement that complied with the IS: 8112 [43] standard. The BFSA used in the study was obtained from Ambala city, India. Various laboratory tests were conducted to determine the properties of both the cement and BFSA. These tests included measurements of normal consistency (28%), soundness (2.5mm), fineness (2%), initial setting time (126 minutes), final setting time (243 minutes), specific

gravity SG (3.19), and CS. The compressive strength of the cement was found to be 26.6, 34.23, and 45.60 MPa at 3, 7, 28 days respectively. Specifications for the mechanical behavior of ordinary coarse aggregate and BFSA has been shown in table 1. For fine aggregate and CAs, natural aggregates were sourced from local markets and underwent grading analysis following the Indian standard IS: 383 [44]. The BFSA used in the study was processed into coarse aggregate shape using a jaw crusher. Additionally, RCS was obtained for the study by manually crushing 5 to 7-month-old uncontaminated concrete cubes (150 mm^3) with a hammer. During the concrete casting process, tap water was utilized after purification to eliminate any harmful substances, adhering to the guidelines specified in IS: 10500-2012 [45].

The comparison of properties between BFSA and normal coarse aggregate revealed some noteworthy differences. These comparisons provide valuable insights into the distinctive characteristics and properties of the two types of aggregates. Such knowledge can aid in the appropriate selection of materials for various construction applications.

Table 1. Specifications for the mechanical behavior of ordinary coarse aggregate and BFSA

Property	Normal coarse aggregate	Blast furnace slag aggregate
Fineness modulus	7.38	7.25
Flakiness index (%)	15.39	7.35
Bulk density(compact) (kg/m3)	1565	1417
Los Angeles abrasion resistance (%)	22.56	35.45
Impact value (%)	9.60	17.30
Bulk density(loose) (kg/m3)	1485	1310
Crushing value (%)	20.10	12.53
Elongation index (%)	10.31	18.65
Specific gravity	2.67	2.58

3. Experimental Design

To optimize the concrete mixture and analyze the experimental data, a CCD of RSM was employed. This design enables the generation of precise optimum values and a comprehensive explanation of the experimental data. The CCD is a well-known experimental design that offers flexibility in selecting the number of center points and axial distances. In this study, Design Expert-13 software was used for 25 mixes experimental runs were conducted using the CCD. In this study, we used 3 center points for a balance of accuracy and efficiency. For more complex systems or higher precision, you can opt for 4 or 5 center points. These runs involved varying amounts of cement, sand, RCS, BFSA, and CA, as detailed in Table 1. The mixture proportions were based on the M25 concrete mix design specified in IS 456:2000 [46]. The independent parameters considered in the study were BFSA and RCS shown in table 2.

Table 2. Independent parameters

Factor	Name	Minimum	Maximum	Coded Low	Coded High	Mean	Std. Dev.
A	RCS (%)	0	100.00	-1	+1	52.00	33.32
B	BFSA(%)	0	50.00	-1	+1	26.00	15.94

Table 3. Mix design with replacement

Level	S No.	RCS(%)	BFSA(%)	Cement (kg/m³)	fine aggregate (kg/m³)	RCS (kg/m³)	CA (kg/m³)	BFSA (kg/m³)	Water (kg/m³)	Extra water (%)
0	0R0B	0	0	342	711.4	0	1174	0	153.9	0
1	10R5B	10	5	342	640.26	71.14	1115.3	58.7	153.9	1
2	25R5B	25	5	342	533.55	177.85	1115.3	58.7	153.9	1
3	50R5B	50	5	342	355.7	355.7	1115.3	58.7	153.9	1
4	75R5B	75	5	342	177.85	533.55	1115.3	58.7	153.9	1
5	100R5B	100	5	342	0	711.4	1115.3	58.7	153.9	1
1	10R15B	10	15	342	640.26	71.14	997.9	176.1	153.9	2
2	25R15B	25	15	342	533.55	177.85	997.9	176.1	153.9	2
3	50R15B	50	15	342	355.7	355.7	997.9	176.1	153.9	2
4	75R15B	75	15	342	177.85	533.55	997.9	176.1	153.9	2
5	100R15B	100	15	342	0	711.4	997.9	176.1	153.9	2
1	10R25B	10	25	342	640.26	71.14	880.5	293.5	153.9	5
2	25R25B	25	25	342	533.55	177.85	880.5	293.5	153.9	5
3	50R25B	50	25	342	355.7	355.7	880.5	293.5	153.9	5
4	75R25B	75	25	342	177.85	533.55	880.5	293.5	153.9	5
5	100R25B	100	25	342	0	711.4	880.5	293.5	153.9	5
1	10R35B	10	35	342	640.26	71.14	763.1	410.9	153.9	6
2	25R35B	25	35	342	533.55	177.85	763.1	410.9	153.9	6
3	50R35B	50	35	342	355.7	355.7	763.1	410.9	153.9	6
4	75R35B	75	35	342	177.85	533.55	763.1	410.9	153.9	6
5	100R35B	100	35	342	0	711.4	763.1	410.9	153.9	6
1	10R50B	10	50	342	640.26	71.14	587	587	153.9	8
2	25R50B	25	50	342	533.55	177.85	587	587	153.9	8
3	50R50B	50	50	342	355.7	355.7	587	587	153.9	8
4	75R50B	75	50	342	177.85	533.55	587	587	153.9	8
5	100R50B	100	50	342	0	711.4	587	587	153.9	8

Ranking: 1 (Very Low), 2 (Low), 3 (High), 4 (Very High), 5 (Extreme)

The mix design for M25 grade concrete followed the Indian Standard, as indicated in the provided table 3. These parameters were carefully adjusted to analyze their effects. The response parameters, denoted as R1, R2 and R3 corresponded to split tensile strength flexural strength and bond strength after 28 days of curing, respectively.

The study involved manipulating specific factors within defined ranges to assess their impact on the concrete's performance. The two factors, RCS (Recycled Concrete Sand) and BFSA (Blast Furnace Slag Aggregate), were varied systematically. RCS ranged from 0% to 100%, while BFSA ranged from 0% to 50%, with both factors assigned coded values of -1 (low) and +1 (high). The mean and standard deviation for RCS were 52.00 %and 33.32%, respectively, while for BFSA, they were 26.00% and 15.94%.

These carefully selected parameters enabled the analysis of their influence on response parameters (R1, R2, and R3) representing split tensile strength, flexural strength, and bond strength after a 28-day curing period.

4. Experimental Procedure

The experimental designs for all 25 runs, including the control mix, were generated using Design Expert 13, as depicted in Table 3. Each individual run involved the manual mixing of concrete with waste materials and water to ensure a homogeneous mixture. The C, fine aggregate, and coarse aggregate were mixed slowly for two minutes, and water was added gradually to achieve the desired workable consistency. Once the suitable mixture was obtained, it was transferred into lubricated molds and uniformly compacted using a table vibrator.

(a) Split Tensile Test setup (b) Flexural test setup (c) Prepared sample for bond test

Fig. 1. Experimental setup

The freshly mixed concrete specimens were then subjected to testing according to the relevant Indian standard codes of practice. The tests included measuring the CS, split tensile strength flexural strength, and concrete-steel tensile bond after 28 days of submersion in water at 27°C. The cube specimens were tested for compressive strength using a Compression Testing Machine (CTM) at the age of 28 days. The testing was conducted without impacts or jerks, applying a uniform load, and recording the failure load

for each specimen. The results obtained from these tests are presented in Figure 1. For the ST and flexural strength test, the same CTM machine was used, as the hydraulic arrangement for the flexural test was attached to the CTM. Additionally, a Universal Testing Machine (UTM) was utilized for the tensile bond test.

5. Results And Discussion

This section presents the results and discussion of the experimental data and mathematical models for various properties, split tensile strength flexural strength, and bond strength. The models were validated using ANOVA, and the coefficients and response surface plots were interpreted to gain insights into the relationships between variables. The results and discussion shed light on the impact of BFSA and RCS replacement parameters on the properties of construction materials. Furthermore, the effectiveness of RSM based on CCD for modeling and optimizing construction materials is demonstrated throughout the analysis.

5.1. Models Fitting

The regression coefficients in the model are estimated by minimizing the sum of squared errors between the predicted values and the actual values of the response variable. The significance of the model and its individual terms is determined using the F-test and t-test, respectively. Once the model is fitted and validated, it becomes useful for predicting the response variable at any combination of BFSA and RCS replacement percentages within the range of the experiments. Additionally, the model can be utilized to identify the optimal combination of BFSA and RCS replacement percentages that maximize or minimize the desired outcome. The Table 4 provides statistical data for various properties of a material, specifically the coefficient, split tensile strength flexural strength, and bond strength.

Table 4. Fit Statistics split tensile strength flexural strength and bond strength

Coefficient	Split tensile strength	Flexural Strength	Bond strength
Std. Dev.	0.0563	0.1455	0.2493
Mean	4.01	4.40	7.84
C.V. %	1.40	3.30	3.18
R^2	0.9935	0.9718	0.9444
Adjusted R^2	0.9852	0.9359	0.9131
Predicted R^2	0.9534	0.8317	0.8291
Adeq Precision	38.6985	18.2110	19.0167

The standard deviation (SD) for these properties is presented as 0.0563, 0.1455, and 0.2493, respectively. The mean values are 4.01, 4.40, and 7.84 for split tensile strength flexural strength, and bond strength, respectively. The coefficient of variation (CV) is 1.40, 3.30, and 3.18% for the corresponding properties. The Table 4 also includes R^2 values, indicating the degree of correlation between the variables, with high values of 0.9935, 0.9718, and 0.9444. Adjusted R^2 values are provided as 0.9852, 0.9359, and 0.9131, representing a measure of the quality of the model fit. Additionally, predicted R^2 values are given as 0.9534, 0.8317, and 0.8291, indicating the predictive power of the model. Finally, precision values are provided as 38.6985, 18.2110, and 19.0167, which represent the precision of the model's predictions for the respective properties.

5.2 Coded Factors

Tables 5 and 6 present the regression equations in terms of coded factors for all responses. The equations express the relationship between the coded factors (represented as A and B) and the dependent variable (denoted as C). The coefficients assigned to the coded

factors determine their impact on the dependent variable. The final equation in Table 5 is derived from the analysis and showcases how the values of the coded factors are combined to determine the value of the dependent variable. It is important to note that for a linear interaction between variables and responses, at least one regression coefficient in the model should not be zero. The experimental data suggests that the relationships between factors and response variables are different for the three strength measures. Split Tensile Strength and Flexural Strength share similar factors, indicating consistent effects across these two measures, while Bond Strength is characterized by cubic terms, suggesting a more intricate and nonlinear relationship with the experimental factors.

The specific reasons for these patterns would likely be influenced by the nature of the materials, the experimental design, and the physical phenomena being studied. The notable observation is that Split Tensile Strength and Flexural Strength exhibit shared factors, signifying a coherent impact across these two measures. In contrast, Bond Strength presents itself with cubic terms, signifying a more complex and nonlinear connection with the experimental factors.

Table 5: Final equation in terms of coded factors

Factors	Split Tensile Strength	Flexural Strength	Bond Strength
	4.03	4.24	8.46
A	-0.0256	0.1114	0.4279
B	6.2	7.97	-4.18
AB	-0.1481	-0.8407	0.2634
A^2	-0.3402	-0.1536	-0.8318
B^2	41.13	52.11	-6.61
A^2B	-0.0597	0.1005	-0.1088
AB^2	-0.5976	-2.73	-0.0669
A^3	0.1891	-0.0087	0.1688
B^3	66.76	81.76	-1.35
A^2B^2	-0.0486	0.0617	
A^3B	-0.0041	-0.0193	
AB^3	-0.414	-1.93	
A^4	-0.0319	0.0104	

Table 6. Actual equation in terms of coded factors

Factor	Split Tensile Strength	Flexural Strength	Bond Strength
	3.18485	3.36335	6.38704
RCS	0.052185	0.020932	0.082
BFSA	-0.02874	0.03658	0.089552
RCS * BFSA	-0.00023	-0.00094	0.000492
RCS^2	-0.00176	-0.00026	-0.00197
$BFSA^2$	0.011599	0.010551	-0.00099
RCS^2 * BFSA	1.59E-06	1.11E-06	-3.48E-06
RCS * $BFSA^2$	0.000012	0.000047	-1.07E-06
RCS^3	0.000021	-2.00E-06	0.000011
$BFSA^3$	-0.00047	-0.00052	-1.1E-05
RCS^2 * $BFSA^2$	-3.11E-08	3.95E-08	
RCS^3 * BFSA	-5.29E-09	-2.46E-08	
RCS * $BFSA^3$	-1.32E-07	-6.16E-07	
RCS^4	-8.17E-08	2.67E-08	
$BFSA^4$	5.04E-06	5.93E-06	

5.3. Splitting tensile Strength (STS) Optimization

5.3.1. Linear Model Fit Summary and ANOVA Evaluation for Split Tensile Strength

The identification of the response surface model was assisted by the model statistics summary and ANOVA for the linear model for split tensile strength as presented in Table 6, respectively. A perfect correlation in the split tensile strength response was observed. The Table 7 includes the sources of variation, the sum of squares, degrees of freedom, mean square, F-value, and p-value for each factor.

The model is found to be significant with a sum of squares of 5.30, 14 degrees of freedom, a mean square of 0.3787, an F-value of 119.54, and a p-value of less than 0.0001. Among the individual factors, B-BFSA has a significant effect on the split tensile strength with a sum of squares of 0.1628, a mean square of 0.1628, an F-value of 51.38, and a p-value of less than 0.0001. A^2 and B^2 also show significant effects on the split tensile strength with corresponding sum of squares, mean squares, F-values, and p-values indicating their significance.

The remaining factors and interactions do not show significant effects on the split tensile strength as indicated by their non-significant F-values and p-values. The residual sum of squares is 0.0348, and the total sum of squares is 5.34.

Table 7. ANOVA for split tensile strength

Source	Sum of Squares	df	Mean Square	F-value	p-value	
Model	5.30	14	0.3787	119.54	< 0.0001	significant
A-RCS	0.0006	1	0.0006	0.1865	0.6742	
B-BFSA	0.1628	1	0.1628	51.38	< 0.0001	
AB	0.0007	1	0.0007	0.2179	0.6498	
A^2	0.0513	1	0.0513	16.19	0.0020	
B^2	0.2766	1	0.2766	87.31	< 0.0001	
A^2B	0.0006	1	0.0006	0.1756	0.6833	
AB^2	0.0025	1	0.0025	0.7759	0.3972	
A^3	0.0373	1	0.0373	11.76	0.0056	
B^3	0.2738	1	0.2738	86.43	< 0.0001	
A^2B^2	0.0008	1	0.0008	0.2665	0.6159	
A^3B	0.0001	1	0.0001	0.0213	0.8866	
AB^3	0.0027	1	0.0027	0.8522	0.3757	
A^4	0.0266	1	0.0266	8.41	0.0145	
B^4	0.2260	1	0.2260	71.36	< 0.0001	
Residual	0.0348	11	0.0032			
Cor Total	5.34	25				

5.3.2. Model Graphs and Diagnostic Findings of Split Tensile Strength

Diagnostic findings in design expert typically include statistical tests and numerical measures that assess the model's quality and predictive accuracy. The lack of fit test determines if the model adequately fits the data, while the residual plot identifies patterns or outliers that may indicate problems with the model. Additional measures like RMSE and R-squared assess the model's predictive accuracy.

Figure 2(a) presents a normal plot of residuals for diagnosing model problems. Figure 2(b) compares predicted and actual values, identifying discrepancies and indicating misspecification or missing predictors. Figure 2(c) identifies systematic bias or non-linear relationships, while Figure 2(d) identifies influential observations and evaluates model robustness. Adjustments can be made based on these findings to enhance accuracy and

predictive power. The ANOVA summary for split tensile strength can be found in Appendix 1.

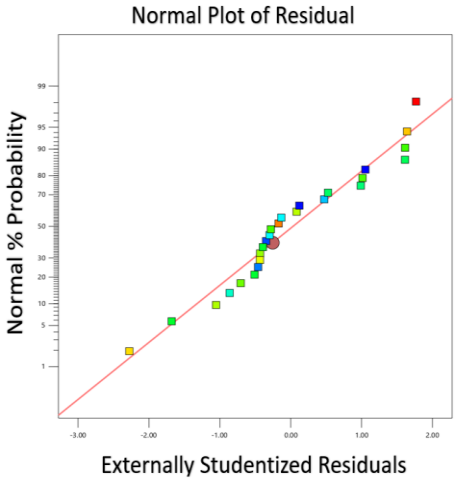

(a) Normal plot of residual

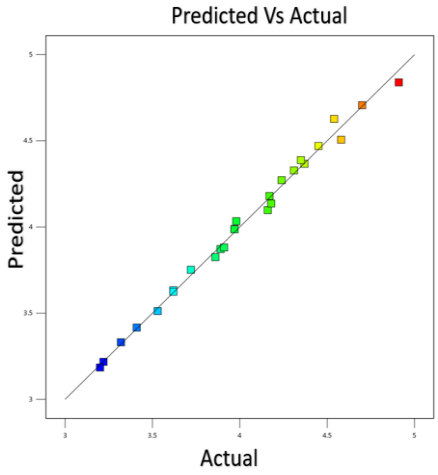

(b) Predicted vs actual

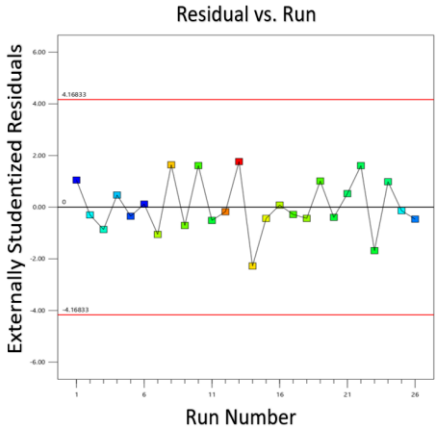

(c) Residual vs run

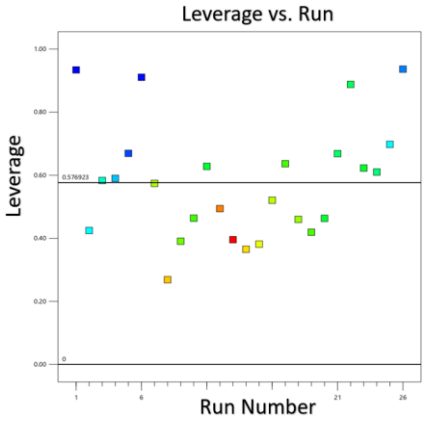

(d) Leverage vs run

Fig. 2. Model graphs and diagnostic findings of split tensile strength

5.3.3. Model Graphs of STS

Model graphs typically include graphical representations of the model, such as contour plots or surface plots, that allow the user to visualize the relationship between the input variables and the response variable. These plots can help identify any nonlinear relationships between the variables and can also help identify any interactions between the variables that may be important for the model.

The relationship between split tensile strength BFSA, and RCS is visualized in Figure 3(a) and 3(b) through contour and 3D plots. The contour plot depicts lines of constant split tensile strength on a grid of BFSA and RCS, while the 3D plot represents split tensile strength on the z-axis and BFSA and RCS on the x and y axes, respectively. By analyzing the contours or the plot's surface, specific regions in the input space can be identified where

split tensile strength is highly responsive to variations in BFSA or RCS. This information facilitates the identification of optimal BFSA and RCS values that minimize split tensile strength or enables an examination of the model's sensitivity to changes in the input variables.

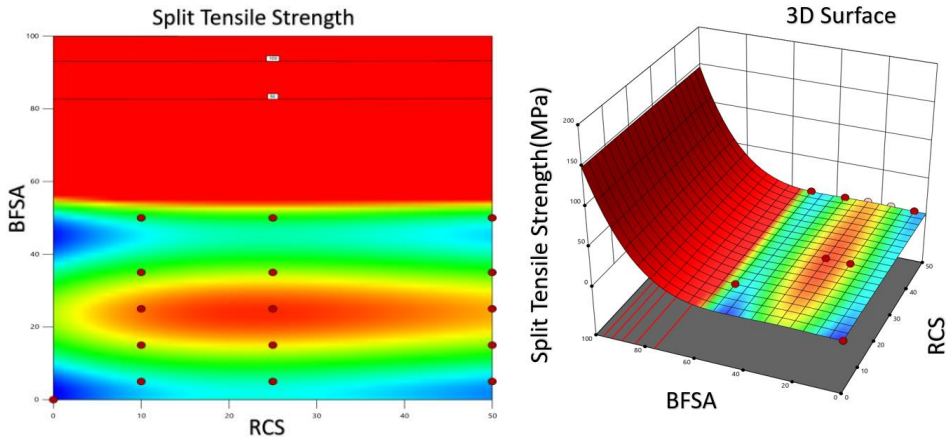

(a) Contour (b) 3D Surface

Fig. 3. Model graphs of split tensile strength

From the above figure 3 its clear that the minimum split tensile strength observed in the dataset is 3.22 MPa, which occurs when there is 100% BFSA replacement and 5% RCS replacement. Conversely, the maximum split tensile strength is 4.91 MPa, observed when there is 25% BFSA replacement and 25% RCS replacement.

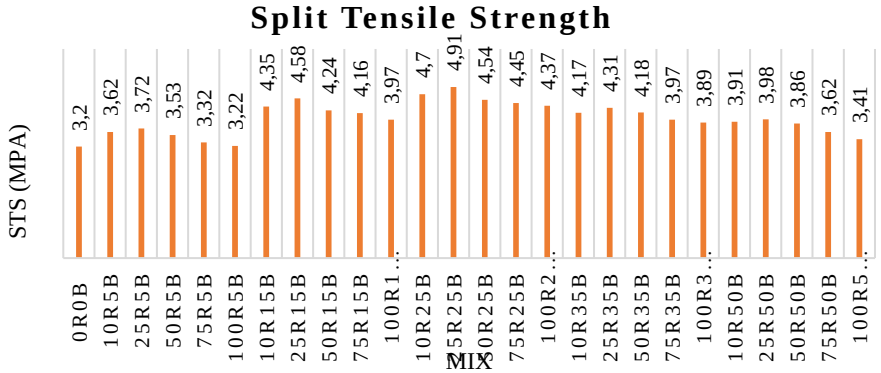

Fig. 4 Split tensile strength values for different concrete mixtures

Figure 4 compares the split tensile strength values of concrete mixtures with varying replacements of fine aggregate by RCS and coarse aggregate by BFSA. The mix labelled "0R0B" represents no replacement of fine aggregate or CA, with a split tensile strength of 3.2 MPa. The Figure reveals the relationship between replacement percentages and split tensile strength values. When both fine aggregate and coarse aggregate replacements are kept constant at 5%, split tensile strength values range from 3.22 (Mix "100R5B") to 3.72 MPa (Mix "25R5B"). This suggests that higher replacement of fine aggregate by RCS does not necessarily lead to a significant decrease in split tensile strength when the coarse

aggregate replacement remains consistent. In terms of coarse aggregate replacement by BFSA, an increase in the replacement percentage from 5 to 25% generally results in higher STS. For example, split tensile strength increases from 4.35 MPa (Mix "10R15B") to 4.91 MPa (Mix "25R25B"). However, when the replacement percentage of coarse aggregate by BFSA reaches 35 and 50%, there is a noticeable decreasing trend in STS. As the coarse aggregate replacement increases, the split tensile strength gradually decreases, with values dropping from 4.18 MPa (Mix "50R35B") to 3.41 MPa (Mix "100R50B").

5.4 Flexural Strength Optimization

5.4.1. Linear Model Fit Summary and ANOVA Evaluation for Flexural Strength

Table 8 presents the results of an ANOVA (Analysis of Variance) model for flexural strength on different sources of variation, including the sum of squares, degrees of freedom (df), mean squares, F-values, and p-values. The objective is to determine the significance of each factor in influencing the FS. The model is found to be significant, with a sum of squares of 8.03, 14 degrees of freedom, a mean square of 0.5734, an F-value of 27.09, and a p-value of less than 0.0001. The table 7 further breaks down the sources of variation, including the factors and their interactions. The factors considered in this analysis are denoted as A-RCS (fine aggregate replacement by RCS) and B-BFSA (coarse aggregate replacement by BFSA). The interactions between these factors are denoted as AB.

Table 8. ANOVA model for flexural strength

Source	Sum of Squares	df	Mean Square	F-value	p-value	
Model	8.03	14	0.5734	27.09	< 0.0001	significant
A-RCS	0.0112	1	0.0112	0.5296	0.4820	
B-BFSA	0.2694	1	0.2694	12.73	0.0044	
AB	0.0222	1	0.0222	1.05	0.3274	
A^2	0.0105	1	0.0105	0.4942	0.4967	
B^2	0.4441	1	0.4441	20.98	0.0008	
A^2B	0.0016	1	0.0016	0.0746	0.7899	
AB^2	0.0512	1	0.0512	2.42	0.1480	
A^3	0.0001	1	0.0001	0.0038	0.9523	
B^3	0.4107	1	0.4107	19.40	0.0011	
A^2B^2	0.0014	1	0.0014	0.0645	0.8042	
A^3B	0.0015	1	0.0015	0.0692	0.7973	
AB^3	0.0584	1	0.0584	2.76	0.1250	
A^4	0.0028	1	0.0028	0.1346	0.7207	
B^4	0.3139	1	0.3139	14.83	0.0027	
Residual	0.2328	11	0.0212			
Cor Total	8.26	25				

It indicates whether each factor or interaction is statistically significant based on the corresponding p-values. It can be observed that the factor B-BFSA has a significant effect on flexural strength, as it has a sum of squares of 0.2694, a mean square of 0.2694, an F-value of 12.73, and a p-value of 0.0044. In summary, the Table 7 provides a comprehensive analysis of the ANOVA model for flexural strength, indicating the significance of the overall model and the effects of different factors and interactions on the flexural strength of the tested samples. interactions do not show significant effects on flexural strength, as their p-values are higher than the significance level (typically 0.05).

5.4.2. Model Graphs and Diagnostic Findings

Design expert provides diagnostic findings that assess the quality of statistical models. These include statistical tests and numerical measures. For instance, the lack of fit test determines if the model adequately fits the data, while the residual plot identifies patterns or outliers that may indicate model issues. Other findings assess predictive accuracy, such as RMSE and R-squared. Users can analyze these diagnostic findings to evaluate model performance, adjust, and enhance accuracy and predictability.

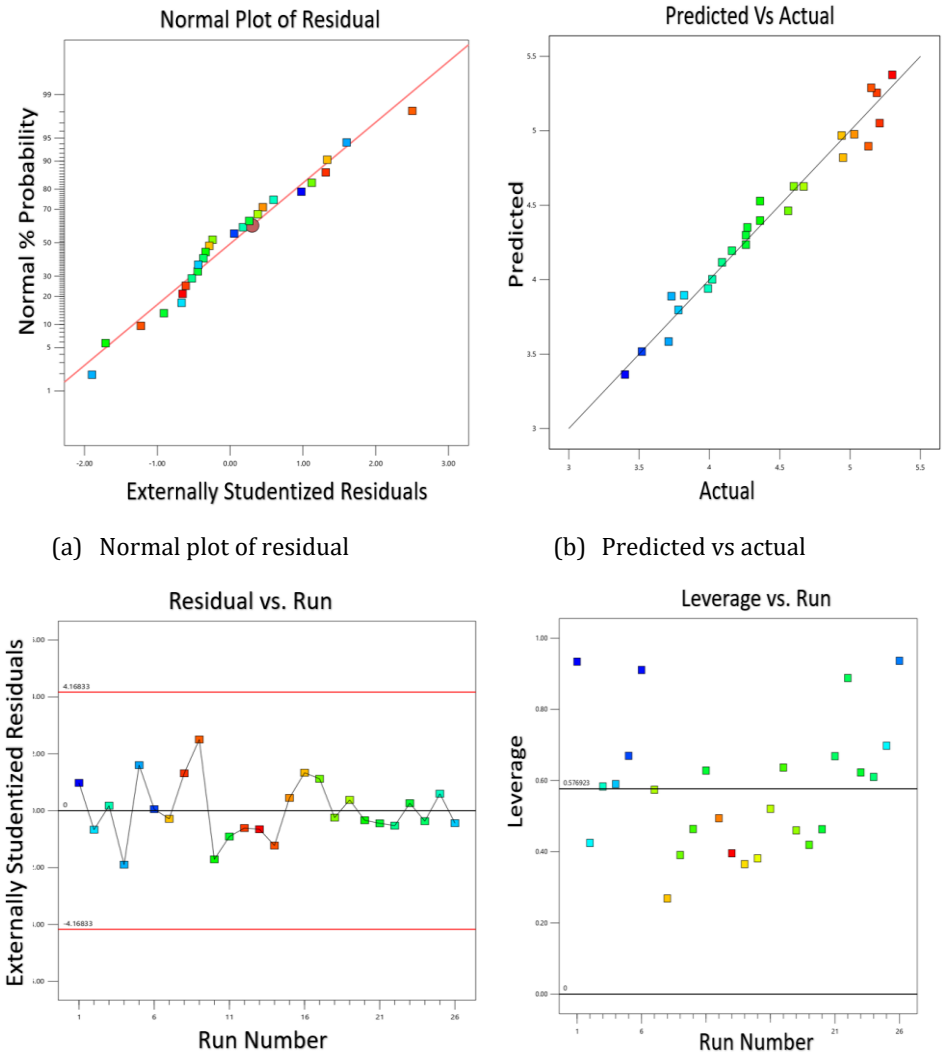

(a) Normal plot of residual (b) Predicted vs actual

(c) Residual vs run (d) Leverage vs run

Fig. 5. Model graphs and diagnostic findings of flexural strength

Figure 5(a) presents a normal plot of residuals, allowing for the diagnosis of problems in a statistical model. Departures from normality in the plot suggest potential issues such as a mis specified model or missing predictors. In Figure 5(b), a predicted vs actual plot compares predicted values to actual values. Deviations from the diagonal line indicate

discrepancies between predicted and actual values, indicating potential model misspecification or missing predictors. Figure 5(c) demonstrates how a predicted vs actual plot can identify systematic bias or non-linear relationships. Figure 5(d) utilizes a leverage vs run plot to identify influential observations and assess model robustness over time or other variables. If influential observations are detected, the model may require re-evaluation or the exclusion of those observations. Additionally, a residual vs run plot can identify trends or cycles in residuals, indicating the need for additional predictors to update the model. These plots contribute to improving the accuracy and predictive power of the model.

5.4.3. Model Graphs of Flexural Strength

Model graphs typically include graphical representations of the model, such as contour plots or surface plots, that allow the user to visualize the relationship between the input variables and the response variable. These plots can help identify any nonlinear relationships between the variables and can also help identify any interactions between the variables that may be important for the model.

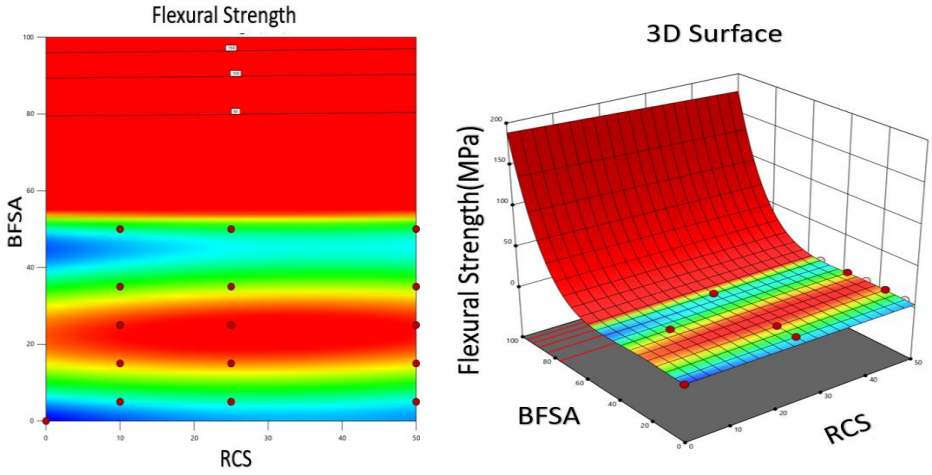

(a) Contour (b) 3D Surface

Fig. 6. Model graphs of Flexural Strength

Contour plots and 3D plots offer visualizations of the relationship between flexural strength, BFSA, and RCS in figure 6(b). In a contour plot, constant flexural strength lines are displayed on a 2D grid representing BFSA and RCS in figure 6(a). Each contour line represents a different flexural strength level, and the spacing between lines indicates the rate of change in F as BFSA and RCS vary. In a 3D plot Figure 6(b), flexural strength values are plotted on the z-axis, while BFSA and RCS are plotted on the x-axis and y-axis. It can be observed that as the percentage of fine aggregate replacement by RCS increases, flexural strength tends to decrease. For example, at 0% RCS replacement, flexural strength is 3.4 MPa, whereas at 100% RCS replacement, flexural strength decreases to 3.52 MPa similarly, flexural strength is affected by the percentage of coarse aggregate replacement by BFSA.

The plot's surface shape depicts the relationship between the variables, with higher flexural strength values corresponding to higher elevations. These plots provide a visual representation of the relationship between flexural strength, BFSA, and RCS. By examining the contours or surface, regions where flexural strength is sensitive to BFSA or RCS changes can be identified. This information aids in determining optimal BFSA and RCS

values to minimize flexural strength or exploring the model's sensitivity to input variable changes.

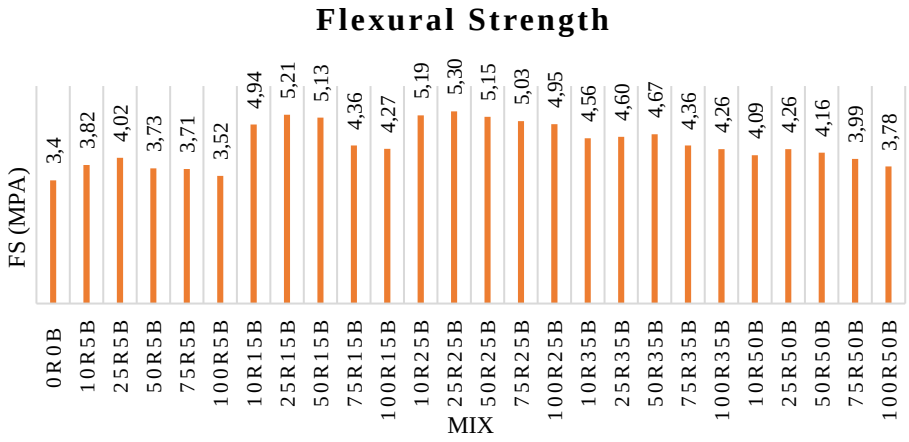

Fig. 7. Flexural strength with different levels of concrete mixture

The Figure 7 provided compares the flexural strength with different levels of fine aggregate replacement by RCS (%) and coarse aggregate replacement by BFSA (%). For each combination of fine aggregate replacement by RCS and coarse aggregate replacement by BFSA, the corresponding flexural strength value is given. It can be observed that as the percentage of fine aggregate replacement by RCS increases, flexural strength tends to decrease. For example, at 0% RCS replacement, flexural strength is 3.4 MPa, whereas at 100% RCS replacement, flexural strength decreases to 3.52 MPa similarly, flexural strength is affected by the percentage of coarse aggregate replacement by BFSA. As the BFSA replacement percentage increases, the flexural strength shows some variations. For instance, at 0% BFSA replacement, the flexural strength is 3.4 MPa, while at 50% BFSA replacement, the flexural strength decreases to 3.73 MPa. The Figure 7 provides a comparison of flexural strength values with different combinations of fine aggregate replacement by RCS and coarse aggregate replacement by BFSA. It helps in understanding the relationship between these replacement percentages and the resulting flexural strength, assisting in the evaluation of suitable aggregate replacement proportions to achieve desired flexural strength levels.

5.5. Bond Strength Optimization

5.5.1. Linear Model Fit Summary and ANOVA Evaluation for Bond Strength

Table 9 displays the analysis of variance (ANOVA) for bond strength, presenting various sources of variation with their sum of squares, degrees of freedom, mean squares, F-values, and p-values. The "Model" row indicates the overall significance of the model, with a sum of squares of 16.88, 9 degrees of freedom, a mean square of 1.88, and an F-value of 30.17. The p-value for the model is less than 0.0001, highlighting its significance. The ANOVA reveals that the overall model fit, represented by the "Model" row, is significant with a small p-value (< 0.0001). The individual factors of fine aggregate replacement by RCS ("A-RCS") and coarse aggregate replacement by BFSA ("B-BFSA") are also found to be significant, with p-values of 0.0462 and 0.0073, respectively. However, the interaction term "AB" and some higher-order terms (A^2B, AB^2, A^3, B^3) are not significant as their p-values are relatively high. The "residual" row captures the unexplained variability in bond

strength after accounting for the factors in the model, while the "Cor Total" row represents the total sum of squares, measuring the overall variability in the bond strength data.

Table 9. ANOVA for bond strength

Source	Sum of Squares	df	Mean Square	F-value	p-value	
Model	16.88	9	1.88	30.17	< 0.0001	significant
A-RCS	0.2904	1	0.2904	4.67	0.0462	
B-BFSA	0.5868	1	0.5868	9.44	0.0073	
AB	0.0171	1	0.0171	0.2753	0.6070	
A^2	1.65	1	1.65	26.58	< 0.0001	
B^2	0.2071	1	0.2071	3.33	0.0867	
A^2B	0.0580	1	0.0580	0.9329	0.3485	
AB^2	0.0017	1	0.0017	0.0267	0.8722	
A^3	1.19	1	1.19	19.17	0.0005	
B^3	0.0176	1	0.0176	0.2832	0.6019	
Residual	0.9947	16	0.0622			
Cor Total	17.88	25				

A more flexible model for capturing non-linear relationships in bond strength data can be achieved by introducing a quadratic term in ANOVA. However, careful consideration of the trade-offs and challenges linked to model complexity and interpretation is necessitated by this approach.

5.5.2. Model Graphs and Diagnostic Findings

Diagnostic findings in Design Expert involve statistical tests and measures to assess model quality. These include the lack of fit test, which evaluates model adequacy, and the residual plot, which detects patterns or outliers that may indicate model issues. Additionally, measures of predictive accuracy like RMSE and R-squared are considered. By examining these findings, users can evaluate model performance, adjust, and enhance accuracy and predictive power. Figure 8(a) provides a normal plot of residuals for diagnosing statistical model problems. In Figure 8(b), a predicted vs actual plot compares predicted values to actual values, highlighting discrepancies that indicate model misspecification or missing predictors. Figure 8(c) identifies systematic bias or non-linear relationships using a predicted vs actual plot. Figure 8(d) uses a leverage vs run plot to identify influential observations and assess model robustness.

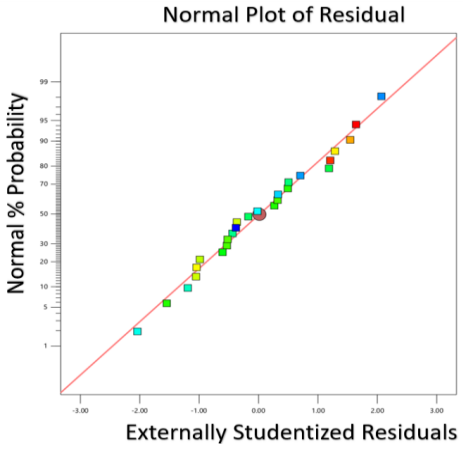

(a) Normal plot of residual

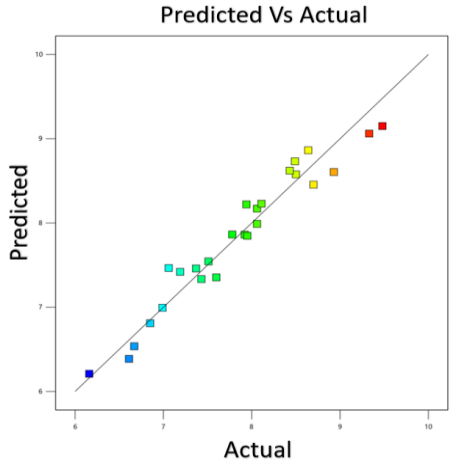

(b) Predicted vs actual

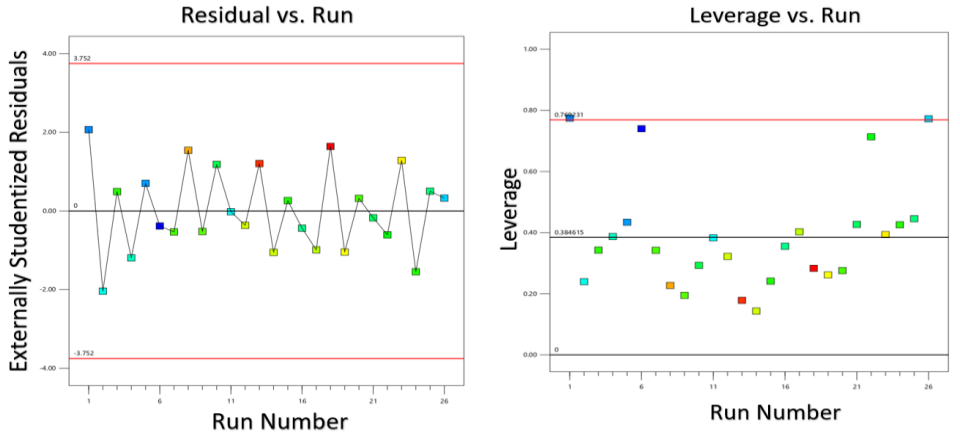

(c) Residual vs run (d) Leverage vs run

Fig. 8. Model graphs and diagnostic findings of bond strength

If influential observations are found, the model may require re-evaluation or exclusion. A residual vs run plot can detect trends or cycles in residuals, indicating the need for additional predictors. These plots enhance model accuracy and predictive power.

5.5.3. Model Graphs of Bond Strength

Model graphs typically include graphical representations of the model, such as contour plots or surface plots, that allow the user to visualize the relationship between the input variables and the response variable. These plots can help identify any nonlinear relationships between the variables and can also help identify any interactions between the variables that may be important for the model.

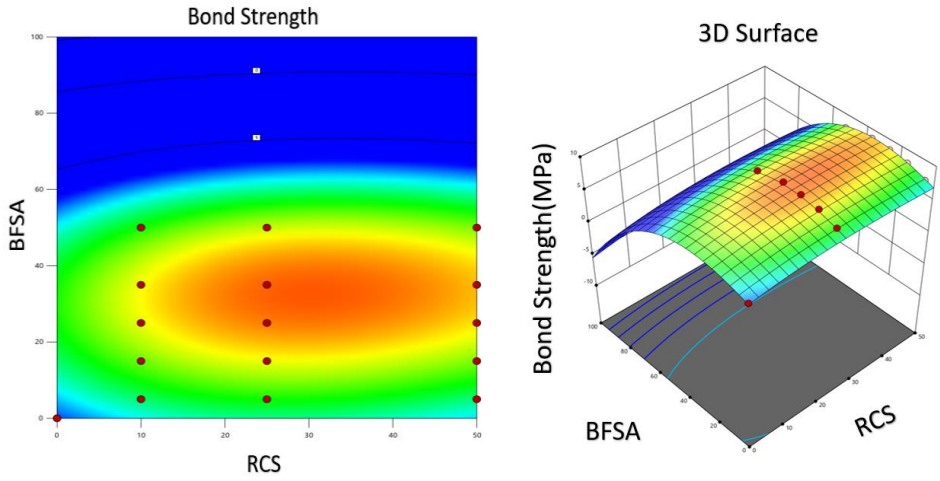

(a) Contour (b) 3D Surface

Fig. 9 Model graphs of bond strength

Figure 9. (a) shows a contour plot and a 3D plot visualize the relationship between bond strength, BFSA, and RCS. Figure 9 (b) shows, lines of constant bond strength are shown on

a grid of BFSA and RCS values. Each contour line represents a different bond strength level, with the spacing indicating the rate of change with varying BFSA and RCS. In a 3D plot, bond strength is plotted on the z-axis, while BFSA and RCS are on the x-axis and y-axis. The plot's surface shape illustrates the relationship, with higher bond strength values corresponding to higher elevations. The minimum bond strength observed in the data is 6.16, which occurs when RCS is replaced by 100% and BFSA by 5%. This suggests that using a higher percentage of replacement for RCS and a lower percentage for BFSA results in a weaker bond strength between the concrete components.

The maximum bond strength recorded is 9.48, occurring when RCS is replaced by 25% and BFSA by 35%. This indicates that a balance between the replacement percentages of both RCS and BFSA can lead to the highest bond strength between the components of the concrete mixture. These plots help identify regions where bond strength is sensitive to BFSA or RCS changes. Optimal BFSA and RCS values can be determined to minimize bond strength or explore sensitivity to input variables.

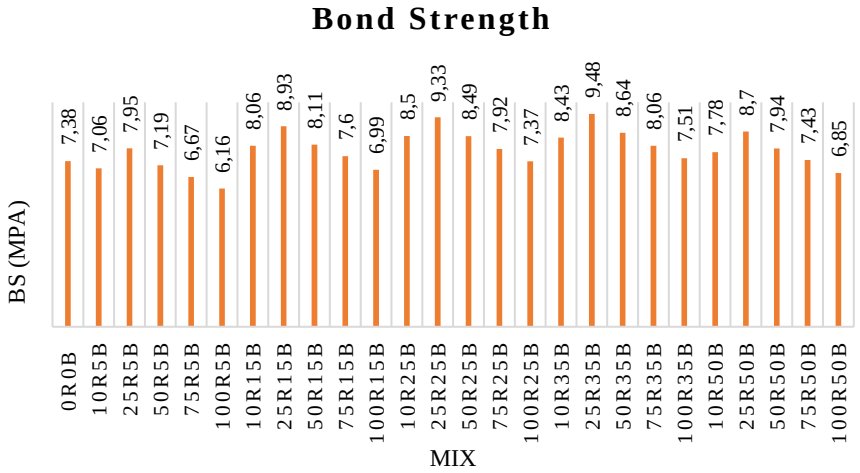

Fig. 10. Bond strength values for different mixes

Figure 10 provides bond strength values for different concrete mixes, indicating the percentages of fine aggregate replacement by RCS and coarse aggregate replacement by BFSA. Each mix is identified by a code consisting of the RCS and BFSA percentages, along with a mix number. The bond strength values represent the strength of the bond between components in each mix. Higher values indicate stronger bonds, while lower values indicate weaker bonds. Increasing the percentage of fine aggregate replacement by RCS generally leads to a decrease in bond strength. For example, comparing mix 0R0B (no replacement) with mix 100R5B, the bond strength decreases from 7.38 to 6.85 MPa. The percentage of coarse aggregate replacement by BFSA does not follow a consistent pattern in relation to bond strength. For instance, mix 10R5B and mix 10R35B both have a 5% BFSA replacement, but their bond strength values differ 7.06 and 8.43 MPa, respectively. Varying the coarse aggregate replacement while keeping the fine aggregate replacement constant can result in different bond strength values. For example, in mix series 10R15B, the bond strength increases as the BFSA replacement increases from 5 to 35%. Figure 10 allows for comparing bond strength values across mixes with varying percentages of RCS and BFSA replacements, providing insights into the impact of these replacements on overall bond strength. therefore, the combination of 25% fine aggregate replacement by RCS and 25% coarse aggregate replacement by BFSA results in the highest bond strength

value of 9.33. This composition seems to offer the optimal balance between the materials, leading to enhanced bond strength in the concrete mixture.

Certain concrete mixtures incorporating Blast Furnace Slag Aggregate and Recycled Concrete sand excel due to BFSA enhancing bonding, countering strength reduction from increased replacements, and enabling properties like traditional concrete. While higher RCS content increased voids and water absorption, BFS helped manage these effects by enhancing bonding. This showcases the potential of thoughtful mixture design with BFSA and RCS to optimize concrete quality and performance[47].

6. Conclusion

In the conclusion, specified limits play a vital role in determining the permissible ranges for various parameters involved in the assessment of construction materials. These limits provide essential guidelines for evaluating the values of parameters such as split tensile strength flexural strength, and bond strength. By defining lower and upper limits for each parameter, these limits ensure that the values fall within acceptable ranges and adhere to specific criteria or desired standards. Adhering to these limits is crucial for maintaining the quality, durability, and overall performance of construction materials.
The Alternate split tensile strength parameter, with a lower limit of 3.2 MPa and an upper limit of 4.91 MPa. The desired range for the flexural strength value is represented by the flexural strength parameter, which has a lower limit of 3.4 MPa and an upper limit of 5.3 MPa. Similarly. The bond strength parameter signifies the acceptable range for the bond strength value, with a lower limit of 6.16 MPa and an upper limit of 9.48 MPa. These limits establish the boundaries within which each parameter should ideally fall, ensuring compliance with specific criteria and desired standards. A similar decreasing trend is observed in the split tensile strength as the percentage of coarse aggregate replacement with BFSA increases. The split tensile strength gradually decreases with a higher coarse aggregate replacement. For example, the split tensile strength decreases from 4.18 in mix "50R35B" to 3.41 in mix "100R50B". Likewise, the flexural strength is influenced by the percentage of coarse aggregate replacement with BFSA. As the BFSA replacement percentage increases, variations in the flexural strength are observed. For instance, at 0% BFSA replacement, the flexural strength is 3.4, while at 50% BFSA replacement, the flexural strength decreases to 3.73.

Furthermore, the bond strength values differ when comparing mixes with the same fine aggregate replacement by RCS but varying coarse aggregate replacement by BFSA. For instance, mix 10R5B and mix 10R35B both have a BFSA replacement of 5%, but their bond strength values differ (7.06 and 8.43, respectively). In mix series 10R15B, the bond strength increases as the BFSA replacement increases from 5 to 35%, indicating the impact of coarse aggregate replacement on bond strength values. These observations highlight the influence of replacing coarse aggregate with BFSA on the mechanical properties of the concrete mixes, such as, split tensile strength flexural strength, and bond strength. It is essential to consider the percentage of coarse aggregate replacement carefully to achieve the desired properties and performance in concrete applications.

Declaration of Competing Interest

The author declares that he has no known competing financial interests or personal relationships that could have appeared to influence the work reported in this paper.

References

[1] Pradhan B, Chand S, Chand S, et al. Emerging groundwater contaminants: A comprehensive review on their health hazards and remediation technologies. Groundwater for Sustainable Development. 2023;20:100868. https://doi.org/10.1016/j.gsd.2022.100868

[2] McAllister J. Factors influencing solid-waste management in the developing world. A Plan B Report Submitted. Degree of Master of Science in Geography. 2015;299:1-95.

[3] Evangelista L, de Brito J. Mechanical behaviour of concrete made with fine recycled concrete aggregates. Cement and Concrete Composites. 2007;29:397-401. https://doi.org/10.1016/j.cemconcomp.2006.12.004

[4] Escalante-García JI, Magallanes-Rivera RX, Gorokhovsky A. Waste gypsum-blast furnace slag cement in mortars with granulated slag and silica sand as aggregates. Construction and Building Materials. 2009;23:2851-5. https://doi.org/10.1016/j.conbuildmat.2009.02.032

[5] Russo N, Lollini F. Effect of carbonated recycled coarse aggregates on the mechanical and durability properties of concrete. Journal of Building Engineering. 2022;51:104290. https://doi.org/10.1016/j.jobe.2022.104290

[6] Pacheco-Torgal F. Introduction to the recycling of construction and demolition waste (CDW). In: Pacheco-Torgal F, Tam VWY, Labrincha JA, et al., editors. Woodhead Publ. Ser. Civ. Struct. Eng., Woodhead Publishing; 2013, 1-6. https://doi.org/10.1533/9780857096906.1

[7] Ulubeyli GC, Artir R. Properties of Hardened Concrete Produced by Waste Marble Powder. Procedia - Social and Behavioral Sciences. 2015;195:2181-90. https://doi.org/10.1016/j.sbspro.2015.06.294

[8] Grazia M De, Trottier C, Dantas SRA, et al. Influence of Recycled Concrete Aggregate Type on Rheological Behaviour of Mixtures Proportioned Using the Equivalent Volume Method. Recent Progress in Materials. 2022;4:1-1. https://doi.org/10.21926/rpm.2203017

[9] Zhu F, Yang C, Miao M. Experimental study on the properties of polyvinyl alcohol fiber reinforced cementitious composites with super early strength. Materials Letters. 2023;330:133264. https://doi.org/10.1016/j.matlet.2022.133264

[10] Latif SD. Concrete compressive strength prediction modeling utilizing deep learning long short-term memory algorithm for a sustainable environment. Environmental Science and Pollution Research. 2021;28:30294-302. https://doi.org/10.1007/s11356-021-12877-y

[11] Pulkit K. Effect of stone slurry & recycled aggregate on properties of concrete Waste management. LAP LAMBERT Academic Publishing (2018-10-12). 2018.

[12] Pulkit K, Saini B, Chalak HD. Factors Affecting the Bond Between Substrate-Overlay Material. A Review. Journal of Engineering Science and Technology Review. 2022;15:55-69. https://doi.org/10.25103/jestr.156.08

[13] Pulkit K, Saini B, Chalak H. The influence of interfacial bond between substrate and overlay concrete by Bi-surface Shear Test and Split prism test. Asia-Pacific Journal of Science and Technology,. 2023.

[14] Koelmel J, Prasad MN V, Velvizhi G, et al. Chapter 15 - Metalliferous Waste in India and Knowledge Explosion in Metal Recovery Techniques and Processes for the Prevention of Pollution. In: Prasad MN V, Shih KBT-EM and W, editors., Academic Press; 2016, 339-90. https://doi.org/10.1016/B978-0-12-803837-6.00015-9

[15] Horii K, Tsutsumi N, Kitano Y, et al. Processing and reusing technologies for steelmaking slag. Nippon Steel Technical Report. 2013;805:123-9.

[16] SALIH MA. New geo-polymerization process for high strength alkali-activated binder with palm oil fuel ash and ground granulated blast furnace slag. 2015. https://doi.org/10.1016/j.conbuildmat.2015.05.119

[17] Owaid HM, Hamid RB, Taha MR. A review of sustainable supplementary cementitious materials as an alternative to all-portland cement mortar and concrete. Australian Journal of Basic and Applied Sciences. 2012;6:287-303.
[18] Abhishek P, Ramachandra P, Niranjan PS. Use of recycled concrete aggregate and granulated blast furnace slag in self-compacting concrete. Materials Today: Proceedings. 2020;42:479-86. https://doi.org/10.1016/j.matpr.2020.10.239
[19] Cao Q, Nawaz U, Jiang X, et al. Effect of air-cooled blast furnace slag aggregate on mechanical properties of ultra-high-performance concrete. Case Studies in Construction Materials. 2022;16:e01027. https://doi.org/10.1016/j.cscm.2022.e01027
[20] Qasrawi H. The use of steel slag aggregate to enhance the mechanical properties of recycled aggregate concrete and retain the environment. Construction and Building Materials. 2014;54:298-304. https://doi.org/10.1016/j.conbuildmat.2013.12.063
[21] Maslehuddin M, Sharif AM, Shameem M, et al. Comparison of properties of steel slag and crushed limestone aggregate concretes. Construction and Building Materials. 2003;17:105-12. https://doi.org/10.1016/S0950-0618(02)00095-8
[22] Yu X, Tao Z, Song T-Y, et al. Performance of concrete made with steel slag and waste glass. Construction and Building Materials. 2016;114:737-46. https://doi.org/10.1016/j.conbuildmat.2016.03.217
[23] Ríos JD, Vahí A, Leiva C, et al. Analysis of the utilization of air-cooled blast furnace slag as industrial waste aggregates in self-compacting concrete. Sustainability (Switzerland). 2019;11. https://doi.org/10.3390/su11061702
[24] Akaözolu S, Ati CD. Effect of Granulated Blast Furnace Slag and fly ash addition on the strength properties of lightweight mortars containing waste PET aggregates. Construction and Building Materials. 2011;25:4052-8. https://doi.org/10.1016/j.conbuildmat.2011.04.042
[25] Habert G. Assessing the environmental impact of conventional and "green" cement production. Eco-Efficient Constr. Build. Mater. Life Cycle Assess. (LCA), Eco-Labelling Case Stud., 2013, 199-238. https://doi.org/10.1533/9780857097729.2.199
[26] Shi J, Tan J, Liu B, et al. Experimental study on full-volume slag alkali-activated mortars: Air-cooled blast furnace slag versus machine-made sand as fine aggregates. Journal of Hazardous Materials. 2021;403. https://doi.org/10.1016/j.jhazmat.2020.123983
[27] Verian KP, Panchmatia P, Olek J, et al. Pavement concrete with air-cooled blast furnace slag and dolomite as coarse aggregates: Effects of deicers and freeze-thaw cycles. Transportation Research Record. 2015;2508:55-64. https://doi.org/10.3141/2508-07
[28] Ahmed T, Ray S, Haque M, et al. Optimization of properties of concrete prepared with waste glass aggregate and condensed milk can fiber using response surface methodology. Cleaner Engineering and Technology. 2022;8:100478. https://doi.org/10.1016/j.clet.2022.100478
[29] Seetharaman R, Seeman M, Kanagarajan D, et al. A statistical evaluation of the corrosion behaviour of friction stir welded AA2024 aluminum alloy. Materials Today: Proceedings. 2020;22:673-80. https://doi.org/10.1016/j.matpr.2019.09.066
[30] Chong BW, Othman R, Jaya RP, et al. Meta-analysis of studies on eggshell concrete using mixed regression and response surface methodology. Journal of King Saud University - Engineering Sciences. 2021.
[31] Manohar DR, Anbazhagan P. Shear strength characteristics of geosynthetic reinforced rubber-sand mixtures. Geotextiles and Geomembranes. 2021;49:910-20. https://doi.org/10.1016/j.geotexmem.2020.12.015
[32] Shi J, Zhao L, Han C, et al. The effects of salinized rubber and nano-SiO2 on microstructure and frost resistance characteristics of concrete using response surface methodology (RSM). Construction and Building Materials. 2022;344:128226. https://doi.org/10.1016/j.conbuildmat.2022.128226

[33] Guo L, Guo Y, Zhong L. Research on the back analysis and failure mechanism of recycled concrete aggregate meso-parameters based on Box-Behnken Design response surface model. Journal of Building Engineering. 2022;51:104317. https://doi.org/10.1016/j.jobe.2022.104317
[34] Ali M, Kumar A, Yvaz A, et al. Central composite design application in the optimization of the effect of pumice stone on lightweight concrete properties using RSM. Case Studies in Construction Materials. 2023;18:e01958. https://doi.org/10.1016/j.cscm.2023.e01958
[35] Mala AA, Sherwani AFH, Younis KH, et al. Mechanical and fracture parameters of ultra-high performance fiber reinforcement concrete cured via steam and water: Optimization of binder content. Materials. 2021;14. https://doi.org/10.3390/ma14082016
[36] Ahmed HU, Mohammed AA, Rafiq S, et al. Compressive strength of sustainable geopolymer concrete composites: A state-of-the-art review. Sustainability (Switzerland). 2021;13. https://doi.org/10.3390/su132413502
[37] Nafees A, Javed MF, Musarat MA, et al. FE Modelling and Analysis of Beam Column Joint Using Reactive Powder Concrete. Crystals. 2021;11. https://doi.org/10.3390/cryst11111372
[38] Peng Y, Ghahnaviyeh MB, Ahamd MN, et al. Analysis of the effect of roughness and concentration of Fe3O4/water nanofluid on the boiling heat transfer using the artificial neural network: An experimental and numerical study. International Journal of Thermal Sciences. 2021;163. https://doi.org/10.1016/j.ijthermalsci.2021.106863
[39] Saboo N, Nirmal Prasad A, Sukhija M, et al. Effect of the use of recycled asphalt pavement (RAP) aggregates on the performance of pervious paver blocks (PPB). Construction and Building Materials. 2020;262:120581. https://doi.org/10.1016/j.conbuildmat.2020.120581
[40] Sinkhonde D. Generating response surface models for optimization of CO2 emission and properties of concrete modified with waste materials. Cleaner Materials. 2022;6:100146. https://doi.org/10.1016/j.clema.2022.100146
[41] Sinkhonde D, Onchiri RO, Oyawa WO, et al. Response surface methodology-based optimisation of cost and compressive strength of rubberized concrete incorporating burnt clay brick powder. Heliyon. 2021;7:e08565. https://doi.org/10.1016/j.heliyon.2021.e08565
[42] Madani T, Boukraa M, Aissani M, et al. Experimental investigation and numerical analysis using Taguchi and ANOVA methods for underwater friction stir welding of aluminum alloy 2017 process improvement. International Journal of Pressure Vessels and Piping. 2023;201:104879. https://doi.org/10.1016/j.ijpvp.2022.104879
[43] IS 8112 - 1989, Specification for 43 grade Ordinary Portland Cement. Bureau of Indian Standards, New Delhi. 2013:17.
[44] IS 383-1970. Specification for coarse and fine aggregates from natural sources for concrete. Bureau of Indian Standard. Published online 1970.
[45] IS 10500. Indian Standard Drinking Water Specification (Second Revision). Bureau of Indian Standards. May 2012;IS 10500:1-11
[46] IS 456. Plain and Reinforced Concrete. Bureau of Indian Standards. Published online 2000.
[47] Lin SK, Wu CH. Improvement of bond strength and durability of recycled aggregate concrete incorporating high volume blast furnace slag. Materials. 2021;14. https://doi.org/10.3390/ma14133708